



NAVAL MEDICAL RESEARCH UNIT SAN ANTONIO

EVALUATION OF AMNION-DERIVED MULTIPOTENT PROGENITOR (AMP) CELLS AND AMNION-DERIVED CELLULAR CYTOKINE SOLUTION (ST266) IN PROMOTING CRANIOMAXILLOFACIAL REGENERATIVE BONE HEALING IN CRITICAL SIZE CALVARIAL DEFECTS

JESSICA M. STUKEL, PhD¹, TEJA GUDA, PhD², MICHELLE E. THOMPSON, DVM³,
RICHARD BANAS, MS⁴, FOREST SHEPPARD, MD, CDR, USN¹,
ALEXANDER J. BURDETTE, PhD^{1*}

- 1) NAVAL MEDICAL RESEARCH UNIT SAN ANTONIO, DEPARTMENT OF EXPEDITIONARY AND TRAUMA MEDICINE, JSBA-FORT SAM HOUSTON, TX
- 2) UNIVERSITY OF TEXAS SAN ANTONIO, DEPARTMENT OF BIOMEDICAL ENGINEERING, SAN ANTONIO, TX
- 3) AIR FORCE MATERIAL COMMAND 711TH HUMAN PERFORMANCE WING, DEPARTMENT OF VETERINARY SCIENCE, JBSA FORT SAM HOUSTON, TX
- 4) NOVESOME BIOTHERAPEUTICS, INC. PITTSBURGH, PA

*CORRESPONDING AUTHOR

DEPARTMENT OF EXPEDITIONARY AND TRAUMA MEDICINE
COMBAT CASUALTY CARE AND OPERATIONAL MEDICINE

NAMRU-SA REPORT # 2018-08

Approved for public release; distribution is unlimited

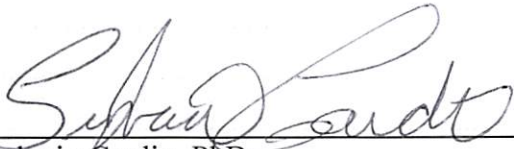
DECLARATION OF INTEREST

The views expressed in this article are those of the authors and do not necessarily reflect the official policy or position of the Department of the Navy, Department of the Army, Department of the Air Force, Department of Defense, nor the U.S. Government. The study protocol was reviewed and approved by the 711th HPW/RHD JBSA-Fort Sam Houston Institutional Animal Care and Use Committee (IACUC) in compliance with all applicable Federal regulations governing the protection of animals in research. This work was supported by funding from: Naval Medical Research Center's Advanced Medical Development Program, work unit number G1507. Dr. Jessica M. Stukel PhD is a contractor. Dr. Alexander J. Burdette PhD is an employee of the US Government. CDR Forest R. Sheppard MD is a Navy military service member and LTC Michelle E. Thompson DVM is an Army military service member. This work was prepared as part of their official duties. Title 17 USC §105 provides that 'copyright protection under this title is not available for any work of the US Government.' Title 17 USC §101 defines a US Government work as a work prepared by a military service member or employee of the US Government as part of that person's official duties.

ACKNOWLEDGEMENTS

We would like to thank Noveome Biotherapeutics for supplying the secretome biotherapeutic [ST266]. The secretome biotherapeutic [ST266] is not FDA approved for any purpose and is still under investigation. We would like to acknowledge Dr. Philip Vernon for intellectual assistance and brainstorming, Dr. Nicholas Hamlin, Mr. Drew Pratt, Mr. Ahmed Metwally, Sergio Montelongo and Mr. Peter Hemond for technical assistance, TSgt Stephanie Carrillo for technical histology assistance, Mr. Darren Fryer and Ms. Kassandra Ozuna for project coordination and Ms. Carrie Crane's veterinary staff for surgical support. We would also like to thank Dr. James Aden for statistical and power analysis assistance and consultation.

REVIEWED AND APPROVED BY:



Sylvain Cardin, PhD
Chair, Scientific Review Board
Chief Science Director
Naval Medical Research Unit San Antonio
3650 Chambers Pass, BLDG 3610
Fort Sam Houston, TX 78234-6315

08 Nov. 2017

Date



CAPT Thomas C. Herzig, MSC, USN
Commanding Officer
Naval Medical Research Unit San Antonio
3650 Chambers Pass, BLDG 3610
Fort Sam Houston, TX 78234-6315

14 Nov 2017

Date

TABLE OF CONTENTS

ABBREVIATIONS	4
EXECUTIVE SUMMARY.....	5
INTRODUCTION	7
MATERIALS AND METHODS	8
RESULTS	14
DISCUSSION	25
MILITARY SIGNIFICANCE.....	30

ABBREVIATIONS

AAALAC	Association for Assessment and Accreditation for Laboratory Animal Care International
AMP	Amnion-derived multipotent progenitor
BCA	Bicinchoninic acid
BS/BV	Bone surface/bone volume
BV/TV	Bone volume/tissue volume
CCC	Combat Casualty Care
CCK-SK	Cell counting kit-SK
DMEM	Dulbecco's modified Eagle's medium
FBS	Fetal bovine serum
FYSA	For your situational awareness
H&E	Hematoxylin and eosin
IACUC	Institutional Animal Care and Use Committee
IGF-1	Insulin growth factor-1
MSC	Mesenchymal stem cell
PBS	Phosphate buffered saline
PDGF-BB	Platelet-derived growth factor beta
RhEGF	Recombinant human epidermal growth factor
ROI	Region of interest
Tb.pf	Trabecular pattern factor
TGF β 2	Transforming growth factor beta 2
TIMP-1	Tissue inhibitor of metalloproteinase-1
TIMP-2	Tissue inhibitor of metalloproteinase-2
VEGF	Vascular endothelial growth factor
μ CT	Microcomputed tomography

EXECUTIVE SUMMARY

Background: Severe traumatic injuries often result in critical size bone defects that are unable to heal without treatment. Autologous grafting is the standard of care but requires additional surgeries for graft procurement, has low bioavailability, high cost and prolonged inpatient care. Alternatives to grafting, such as cell-based and biotherapeutic strategies, aim to address these disadvantages. Amnion-derived multipotent progenitor (AMP) cells release ST266, a secretome of biomolecules identified as integral to the process of bone regeneration and angiogenesis. The AMP cells and secretome are currently under development as biotherapeutics.

Objective: The objective of this study was to determine the regenerative potential of AMP cells and their secretome ST266, in healing critical size bone defects. Additionally, high-throughput gene analytics were utilized to evaluate AMP and ST266-induced gene expression indicative of reparative wound healing to establish a mechanism for observed pro-osteogenic effects.

Methods: The efficacy of ST266 was evaluated *in vitro* by measuring the proliferation and migration of mesenchymal stem cells (MSCs) and osteoprogenitor cells. The ability of AMP cells to undergo osteogenic differentiation was evaluated by mineralization. The proliferation and viability of AMP cells was determined on the Helistat® scaffold *in vitro*. Scaffolds incorporating ST266 or AMP cells were evaluated *in vivo* using a critical size rat calvarial defect model for fluidigm gene analysis at one, two, four, 12 and 24 weeks, and bone regeneration at four weeks, 12 weeks or 24 weeks.

Results: The ST266 enhanced the proliferation and migration of MSCs and the proliferation of osteoprogenitor cells. AMP cells showed osteogenic differentiation by mineralization and with growth and viability on the Helistat® scaffold. ST266 improved new bone volume and connectivity by 12 weeks and significantly improved angiogenesis at four weeks and bone density at four and 12 weeks with no deleterious effects. ST266 was superior to the AMP cells as the AMP cells appeared to inhibit bone formation. Fluidigm gene analysis showed up-regulation of osteogenic-related genes over time in all groups, but no significant differences between groups.

Conclusions: The improvement in new bone volume, connectivity and angiogenesis suggests that the ST266 facilitates bone healing *in vivo*. The *in vitro* analysis suggests that the mechanism of ST266-induced regenerative healing may arise from the proliferative and migratory effects of

ST266 on MSCs and osteoprogenitor cells. Future studies are warranted as a higher dose of ST266 may further improve regeneration.

INTRODUCTION

Despite the regenerative potential of bone for healing small fractures, large critical size bone defects induced by insults such as severe trauma in the civilian and military setting cannot heal on their own. Such large defects can occur not only in long bone, but also in the irregular-shaped bones of the craniomaxillofacial region. To date, the clinical standard of care for dealing with such large defects is autologous grafting as this method is fully capable of healing critical size bone defects. However, this technique suffers from substantial disadvantages including additional surgeries, has low bioavailability, high cost and prolonged inpatient care [1, 2]. Therefore, new strategies are being pursued to overcome the problems associated with autologous grafting without sacrificing its beneficial effects.

One potential approach is the use of mesenchymal stem cell- (MSC) based therapeutics. During the course of bone healing, endogenous MSCs are recruited to the injury site, proliferate and differentiate into osteoblasts and begin producing new bone [3]. This process is orchestrated by many different growth factors secreted by the MSCs themselves as well as surrounding cells. Such knowledge has prompted the use of MSCs directly, or the MSC secreted growth factors to regenerate bone. Indeed, several studies have demonstrated the potential of using both MSCs and/or their secreted factors (known as conditioned medium) to regenerate critical size bone defects [4-6]. These two approaches are particularly appealing as MSCs or their conditioned medium can still regenerate critical size bone defects without requiring additional surgeries, is less expensive than autologous grafting and may reduce time of inpatient care. Conditioned medium is especially beneficial as it is not donor specific and can be lyophilized, enabling more practical storage conditions. However, the tissue source that the MSCs are derived from not only influences the types and concentrations of paracrine factors secreted by the MSCs [7], but also differ in the bioavailability of MSCs from that tissue source, as well as their proliferative and immunomodulatory characteristics [8]. This has prompted research into evaluating the bone regenerative abilities of MSCs and their paracrine factors derived from different tissue sources.

Amnion-derived multipotent progenitor (AMP) cells and their conditioned medium, ST266, are two novel therapeutics developed by Stemnion, Inc. that may be useful for regenerating critical size bone defects. AMP cells secrete a number of growth factors including platelet-derived growth factor beta (PDGF-BB), transforming growth factor beta 2 (TGF β 2), vascular endothelial growth factor (VEGF), tissue inhibitor of metalloproteinase-1 (TIMP-1),

tissue inhibitor of metalloproteinase-2 (TIMP-2) and angiogenin [9]. Studies have shown that these growth factors have bone regenerative capabilities and may contribute to regeneration of critical size bone defects through enhancing MSC migration, proliferation and angiogenesis [10-13]. For example, VEGF is a potent inducer of angiogenesis, which is needed to create blood vessels and restore circulation to the defect site [14, 15]. PDGF-BB and TGF enhance bone regeneration by acting as proliferative and chemotactic factors for MSCs which are recruited to the defect site to differentiate into osteoblasts [16, 17]. Finally, TIMP-2 has been shown to induce proliferation in primary rat calvarial osteoblast-like cell cultures, as well as enhance healing in critical size bone defects [11].

In this study, the ability of AMP cells and their conditioned medium, ST266, to enhance regeneration of critical size bone defects is investigated at both the *in vitro* level and the *in vivo* level. The *in vitro* effects of ST266 on proliferation and migration of rat MSCs and calvarial osteoprogenitor cells are examined, as well as the ability of AMP cells to undergo osteogenic differentiation. *In vivo*, the ability of AMP cells and ST266 to induce regeneration of critical size calvarial defects in rats is evaluated through microcomputed tomography (μ CT) and histology, as well as fluidigm gene expression analysis to assess the mechanism of action.

MATERIALS AND METHODS

Subjects

Subjects used in the study include male Fischer 344 (CDF®) rats weighing 280-300 grams obtained from Charles River. The study protocol for a rat calvarial defect model was reviewed and approved by the 711th HPW/RHD JBSA-Fort Sam Houston Institutional Animal Care and Use Committee (IACUC) in compliance with all applicable Federal regulations governing the protection of animals in research. All procedures were performed in facilities accredited by the Association for Assessment and Accreditation for Laboratory Animal Care International (AAALAC).

Procedures

MSC and Calvarial Osteoprogenitor Cell Proliferation/Viability Assays

Proliferation/viability was measured by cell counting kit-SK (CCK-SK) (Dojindo), a water-soluble tetrazolium salt that produces a formazan dye upon reduction by dehydrogenases. The amount of formazan dye (measured by absorbance) is directly proportional to the number of living cells. Rat calvarial osteoprogenitor cells (Lonza) were grown to confluence in accompanying media (Lonza) according to manufacturer instructions and then seeded in a 96-well flat bottom plate at 5,000 cells per well and allowed to adhere for eight hours. The medium was then removed and cells were washed twice with phosphate buffered saline (PBS) and 100 μ l of either ST266 or PBS (negative control) was added to the cells and incubated for 48hr and 72hr at 37°C in a cell culture incubator. PBS was used as the negative control since it is most similar to the negative control (saline) being used in clinical trials. Separate wells were used for the 48hr and 72hr time-point. At the 48hr and 72hr time-points, 10 μ l of CCK-SK was added to each well and incubated at 37°C for one hour. Absorbance of CCK-SK was recorded at 450nm on a Biotek Synergy plate reader to assess cell proliferation/viability.

For proliferation/viability assays of rat bone-marrow derived MSCs, the rat MSCs (Cyagen) were cultured to confluence (three days) according to manufacturer instructions and seeded in a 96-well flat bottom plate at 8,700 cells per well in Dulbecco's modified Eagle's medium/F12 (DMEM/F12) (Life Technologies) containing 10% MSC qualified fetal bovine serum (FBS) and allowed to adhere for eight hours. The cells were washed, treatments were added and the proliferation/viability assay was then carried out as described for rat calvarial osteoprogenitor cells. For all experiments, both cells types were not used beyond passage four.

MSC and Calvarial Osteoprogenitor Cell Migration Assays

Rat calvarial osteoprogenitor cells and rat MSCs were grown to confluence according to manufacturer instructions and then harvested for the cell migration assay using a cell migration kit (CellBiolabs). The treatment (500 μ l of ST266 or PBS (negative control)) was added to the bottom well of the migration assay plate and rat calvarial osteoprogenitor cells were seeded at 150,000 cells per insert in 300 μ l of serum-free medium from Lonza, while rat MSCs were seeded at 125,000 cells per insert in 300 μ l of serum-free DMEM/F12 media. No positive control was used since FBS inhibited migration and other positive control candidates were not

reproducible. The cells were then allowed to incubate for 6hr and 24hr at 37°C in a cell culture incubator. At each respective time-point, the treatment was removed from the bottom well, the media in the insert was removed, migrated cells were detached from the bottom of the insert, lysed and detected by the fluorescent DNA binding dye according to manufacturer instructions.

ST266 Release Kinetics

To evaluate the release kinetics of ST266 from the FDA-approved Helistat® scaffold, 500µl of ST266 was added to an 8mm x 1mm circular scaffold placed into an upside-down 15mL conical cap in a six-well plate. The ST266 was then incubated with the scaffold for 15 minutes (optimal incorporation time determined by preliminary experiments (data not shown)) and the scaffold was transferred to a new 15mL conical cap and 1mL of PBS was added. At each time-point, 1mL of PBS was removed and 1mL of fresh PBS was added. The release kinetics were determined on day one, three, seven and 14. The total protein (in micrograms) released from the scaffold was assessed by a bicinchoninic acid (BCA) assay (Pierce) and expressed as percent released, based upon the amount of ST266 that was incorporated.

Human AMP Cell Scaffold Seeding

AMP cells were thawed and transferred to 9mL of STM100 media containing 20ng/mL of recombinant human epidermal growth factor (rhEGF) (Miltenyi; tissue culture grade) and centrifuged at 1250rpm for 10 minutes at room temperature. The media was removed and cells resuspended in 10mL of fresh STM100 with rhEGF to give a concentration of 1×10^6 cells/mL. Typical recovery rate was >75%. As AMP cells are only viable for two to three population doublings, they were immediately used for cell seeding. To seed the AMP cells on the Helistat® absorbable collagen sponge scaffold (8x1mm), 1mL of AMP cells (1×10^6 cells) was aliquoted to a microcentrifuge tube and spun down at 1250rpm for five minutes to collect cells and then resuspended in 60µl of STM100 with rhEGF. The Helistat® scaffold was placed in an upside-down 50mL conical cap in a six-well plate and 30µl of cells (500,000 cells) were seeded on each side and then allowed to adhere for 1hr at 37°C in a cell culture incubator. After 1hr, 2mL of STM100 with rhEGF were added to the 50mL conical cap and cells were allowed to grow on the scaffold overnight at 37°C in a cell culture incubator.

Assessment of AMP Cell Proliferation/Viability on the Scaffold

The proliferation/viability of AMP cells on the scaffold was assessed by CCK-SK. After the overnight incubation of the AMP cells on the scaffold, the scaffold was transferred to a new well in a six-well plate and 2mL of STM100 media with rhEGF and 200 μ l of CCK-SK was added and allowed to incubate at 37°C in a cell culture incubator for 3hr. Samples of 100 μ l were then diluted 1:1 with PBS before being transferred to a flat bottom 96-well plate. Absorbance was then read at 450nm on a Biotek microplate reader.

Live/Dead Staining of AMP Cells on the Scaffold

AMP cells were seeded and allowed to grow on the scaffold as described above and then 4 μ M of Calcein and 8 μ M of ethidium homodimer-1 were added to the cell-seeded scaffold and incubated for 30 minutes according to manufacturer instructions (Life Technologies). After incubation, live/dead staining of the scaffolds was imaged on a confocal microscope (Nikon).

AMP Cell Differentiation

To determine whether AMP cells can differentiate into osteoblasts, AMP cells were seeded in a 6-well plate at 200,000 cells/cm² in STM100 media with rhEGF and allowed to adhere overnight at 37°C in a cell culture incubator. The next day, the media was removed, cells washed 2x in PBS, and then either STM100 media with rhEGF (controls) or osteogenic differentiation media (Lonza) was added to the cells and allowed to differentiate for 21 days. The media for controls and osteogenic differentiation cells was replaced 3x a week. At the end of 21 days, the media was removed, cells washed 2x in PBS, and fixed in 100% ethanol. Mineralization was then detected by alizarin red staining (CosmoBio).

Rat Calvarial Defect Model

The study protocol was approved by the IACUC at the 711th Human Performance Wing, Joint Base San Antonio-Fort Sam Houston, and conducted in accordance with the Guide for the Care and Use of Laboratory Animals, Institute of Laboratory Animals Resources, National Research Council, National Academy Press, 2011. All procedures were performed in facilities Accredited by the AAALAC.

The rat calvarial defect model was performed as detailed [18]. Male Fischer 344 (CDF®) rats weighing 280-300 grams (10-12 weeks old) obtained from Charles River were used for the study. The rats were anesthetized with isoflurane and then placed into a stereotaxic device (Stoelting). The head was shaved and disinfected with three washes of chlorhexidine soaked gauze. An incision was made through the skin and the periosteum was peeled back from the overlying bone. An 8mm trephine burr was used to score the defect most of the way through the bone with constant saline irrigation to prevent overheating. An elevator was then used to break the rest of the bone disk away from the dura while carefully peeling the underlying dura away from the bone to prevent any damage to it. The treatments were then placed into the defects and rats were randomly assorted into cohorts of (1) untreated empty defects, (2) saline incorporated scaffold, (3) ST266 incorporated scaffold and (4) AMP cell incorporated scaffold. The saline, ST266 and AMP cell cohorts included n=8 per group with n=3 for fluidigm gene expression and n=5 for μ CT and histology. The one and two week cohorts had n=3 per cohort, which were for fluidigm analysis only. After treatment placement, the periosteum and connective tissue was sutured and the skin was sealed up using Vetbond (Patterson Veterinary). The animals were then allowed to heal for one, two, four, 12 or 24 weeks before being euthanized for fluidigm expression, or four, 12 and 24 weeks before being euthanized for μ CT and histology. Buprenorphine (0.1mg/kg; Reckitt & Colman Pharmaceuticals Inc.) was given pre- and post-operatively for pain.

Fluidigm Gene Expression

At the end of the respective healing period, the animals were euthanized by an injection of pentobarbital (1mL/rat) and confirmed by a thoracotomy. The skull cap which incorporated the defect and 1-2mm of surrounding bone was removed for RNA isolation in RNazol RT® (Sigma). The pieces of skull cap were homogenized in 1mL of RNazol RT® and then isolated according to manufacturer instructions and sent for fluidigm gene expression analysis by the University of Texas Health Science Center San Antonio. Data were normalized to the *colla2* housekeeping gene and expressed as fold change by the delta-delta CT method.

Microcomputed Tomography and Histology Evaluation

For μ CT analysis and histology, the animals were euthanized by an injection of pentobarbital (1mL/rat) and followed up by a thoracotomy. The skull cap was then harvested according to [18] and placed in 10% buffered formalin for μ CT analysis. Following harvesting, the samples were scanned using μ CT by a SkyScan 1076 (Bruker, Kontich, Belgium) scanner at 100kV source voltage and 100mA source current with an 0.05mm aluminum filter and a spatial resolution of 8.77 μ m while hydrated with formalin. The images were reconstructed with NRecon software (Skyscan) to generate gray-scale images ranging from zero to 255. A region of interest (ROI) was selected and comprised of the 3D volume that extended over the 8mm defect space created at the time of surgery to a thickness of 1.5mm. The μ CT reconstructed axial slices were then evaluated by using CT software (CTAn, Bruker, Kontich, Belgium) to determine the bone regeneration patterns *in vivo* in terms of cranial-to-caudal bone growth profiles and overall bone volume, bone surface to bone volume ratio, mineral density of regenerated bone and trabecular pattern factor (Tb.pf). Tb.pf incorporates trabecular number, spacing and thickness with lower values indicating greater connectivity. New bone evaluation was based on differences in density between the newly forming osteoid and native bone. To account for individual variability between animals, the density values were normalized by the density of the native calvarial bone outside the ROI.

After μ CT analysis, tissue specimens were decalcified in Cal-Ex IITM Fixative/Decalcifier for 3.5 hours and three sections of each calvarium (cranial, central and caudal) were embedded in paraffin. Tissue blocks were decalcified again overnight after rough cut. Tissue sections were cut at 5 μ m and stained with hematoxylin and eosin (H&E) for histopathologic evaluation. Histologic scoring was performed by a board certified veterinary pathologist. Digital photomicrographs were taken using an Olympus BX51 microscope and an Olympus DP72 camera.

Statistical Analysis

Statistical analysis for proliferation and cell migration assays was performed using the unpaired Holm-Sidak method for multiple comparisons t-test with $p < 0.05$ for significance. For μ CT analysis, a two-way ANOVA with *post hoc* Bonferroni was used with $p < 0.05$ significance. Group comparisons were made between groups and across time. Statistical analysis for

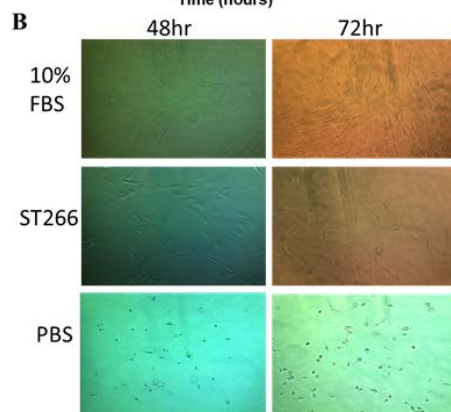
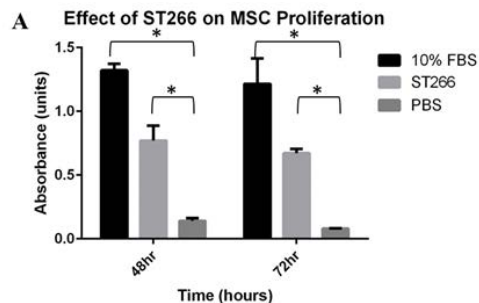
histological scoring was performed as described [19] using the Mann-Whitney test at $p < 0.05$ significance.

RESULTS

MSC and Calvarial Osteoprogenitor Cell Proliferation/Viability Assays

The bioactivity of the ST266 solution with respect to bone regeneration was evaluated for rat bone marrow derived MSCs and rat calvarial osteoblasts. The proliferation studies of ST266 effect on MSC and osteoblast proliferation revealed that ST266 solution enhances the proliferation of both MSCs and calvarial osteoblasts compared to the negative control PBS (Figure 1A) while maintaining normal gross morphology (Figure 1B). Interestingly, ST266 treatment enhanced proliferation of osteoblasts to a similar extent as the positive control which was the nutrient rich growth medium with 10% FBS in DMEM/F12.

MSC Proliferation and Morphology



Osteoblast Proliferation and Morphology

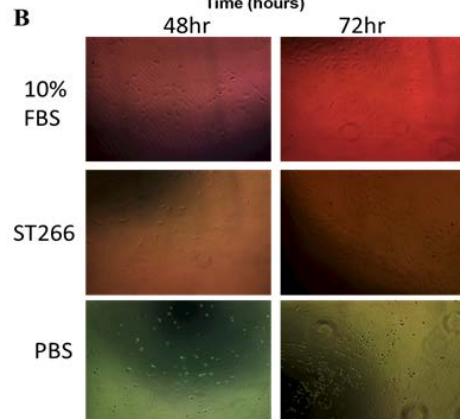
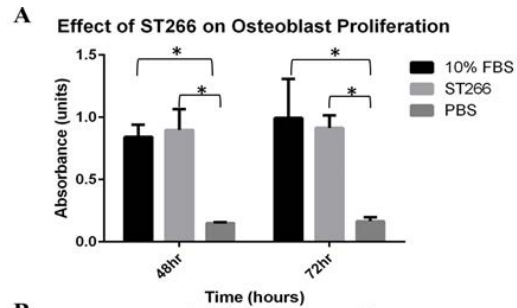
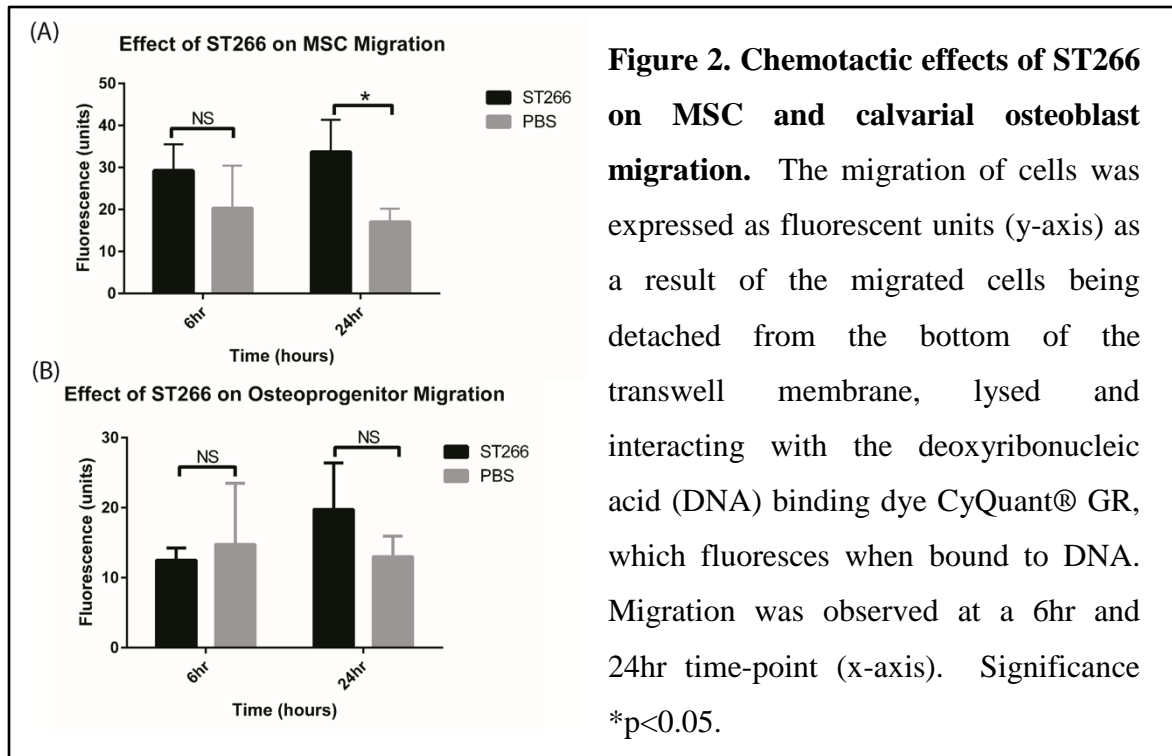


Figure 1. Proliferative and chemotactic effects of ST-266 in rat MSCs and rat calvarial osteoblasts. (A) The ST266 enhances the proliferation of MSCs and osteoprogenitor cells. The proliferation of the cells is shown by the increase in absorbance (y-axis) using the metabolic dye CCK-8. Proliferation was monitored at 48hr and 72hr time-points (x-axis). The 10% FBS treatment represents the reference positive control, which contains DMEM/F12 with 10% MSC- qualified FBS for the MSCs or DMEM with standard 10% FBS for the osteoprogenitor cells. Significance * $p < 0.05$. (B) The cell morphology remained normal when cultured with 10% FBS, ST266 and PBS.

MSC and Calvarial Osteoprogenitor Cell Migration Assays

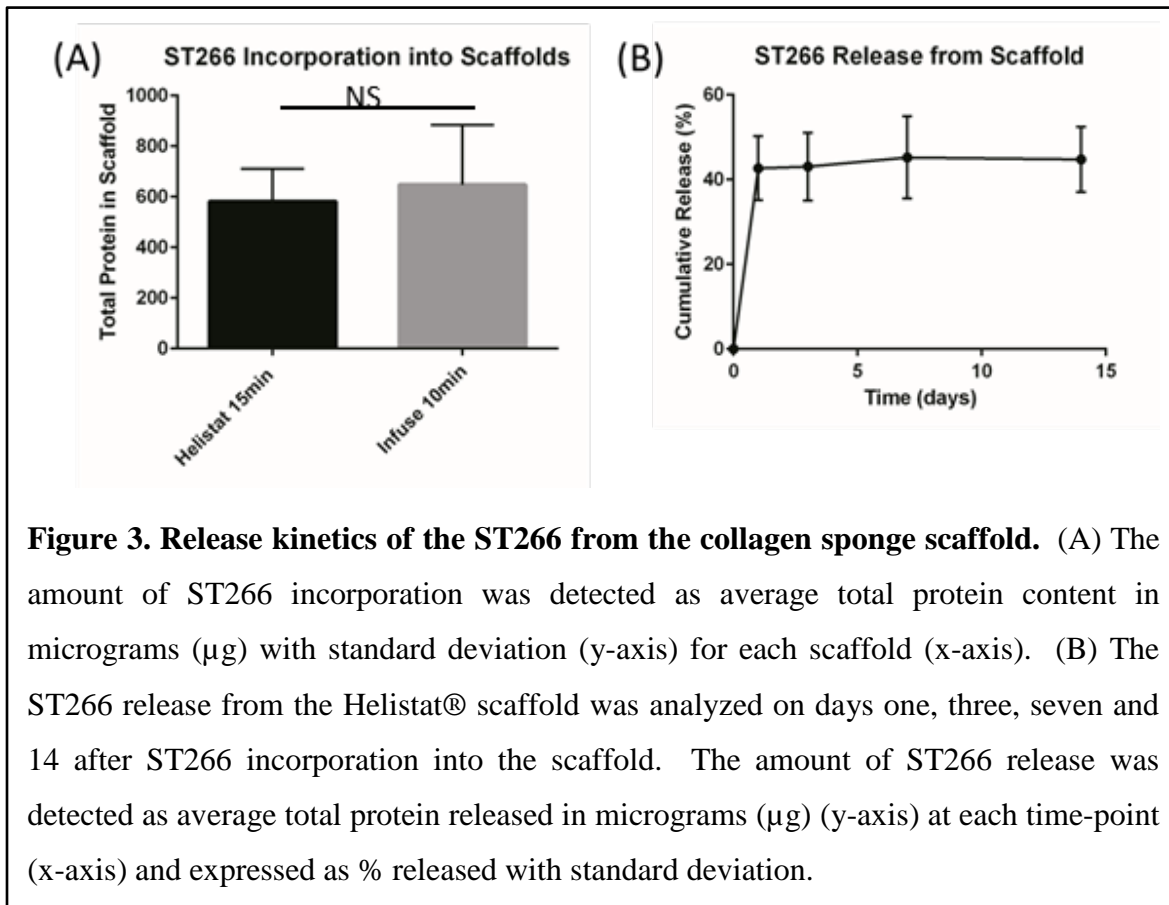
We also evaluated the ability of ST266 treatment to induce migration of MSCs and calvarial osteoblasts. ST266 solution significantly increased migration of MSCs compared to the PBS negative control by 24hr. Additionally, a trend of higher migration was observed in rat calvarial osteoblasts by 24hr, but it was not significant (Figure 2).



ST266 Release Kinetics

The optimal amount of ST266 that can be incorporated and released into two different scaffolds was evaluated and compared to down-selection. When each scaffold was submerged in 500 μ l of ST266 solution for different incubation times, a 10 minute incubation time was determined to be optimal for the INFUSE™ scaffold and a 15 minute incubation was optimal for the Helistat® scaffold (Figure 3A). However, since there was a larger amount of variability for ST266 incorporation into the INFUSE™ scaffold, the Helistat® scaffold was chosen for all subsequent experiments. The average ST266 incorporation amount in the Helistat® scaffold was 500 μ g (50 μ g of ST266 secretome with the rest being a protein stabilizer).

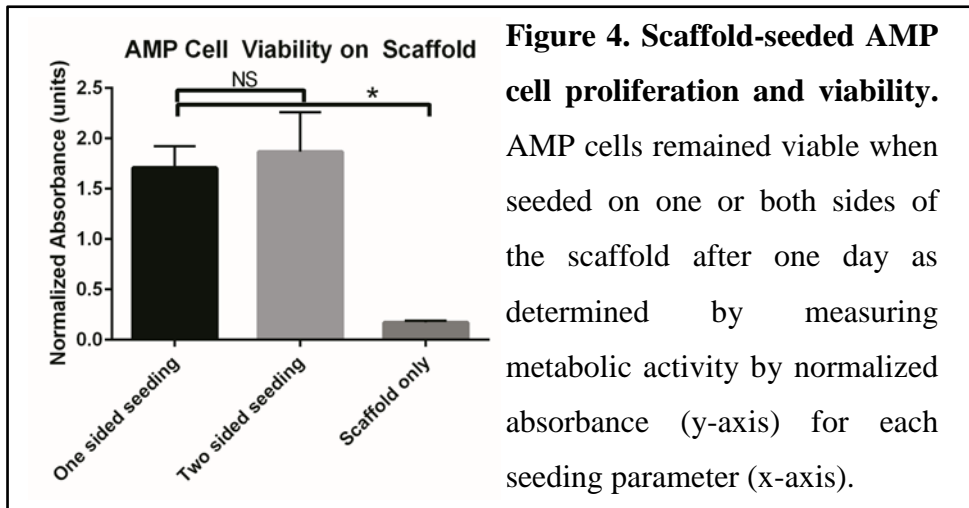
The release kinetics of the ST266 solution from the Helistat® scaffold was then investigated over a 14 day period by measuring total protein release using a BCA assay. Within the first day, almost 50% (24µg of secretome) of the ST266 solution was released from the scaffold (Figure 3B). After that initial burst release however, there was a very slow and gradual release from one day to 14 days. These data demonstrate that the ST266 solution can be incorporated into the Helistat® scaffold and exhibits an initial burst release during the first day, followed by slow release in the following days. Thus, the Helistat® scaffold is suitable for use as a delivery vehicle for the ST266 solution.



Assessment of AMP Cell Proliferation and Viability on the Scaffold

As AMP cells are the source of the ST266 solution, the osteogenic differentiation potential of the AMP cells was analyzed. Preliminary experiments with different cell seeding densities found that a seeding amount of one million cells on the scaffold demonstrated the highest metabolic activity (data not shown). The viability and number of the cells on the scaffold was also analyzed based on seeding one million cells on one side of the scaffold, or

500,000 cells on both sides. As shown in Figure 4, there was not a significant difference in viability between one-sided and two-sided seeding. However, since two-sided seeding allows more thorough distribution of the cells throughout the scaffold, this seeding strategy was utilized for subsequent experiments.



Live/Dead staining of the AMP cells on the scaffold was then performed as a secondary readout for viability, as well as to look at the distribution of cells throughout the scaffold using confocal microscopy with two-sided seeding. As shown in Figure 5, the AMP cells distributed throughout the scaffold with a penetration depth of about 0.5mm (half the scaffold thickness) on the top side (top panels) and bottom side of the scaffold (bottom panels). Many live cells are observed in the scaffold (green; left panels) with only some dead cells (red; right panels). Given that the AMP cells are immediately seeded on the scaffold upon thawing, it is not surprising that there are some dead cells present as cell viability is rarely 100% when thawing frozen cells. Thus, AMP cells can attach, distribute, and maintain viability when seeded on the Helistat® scaffold.

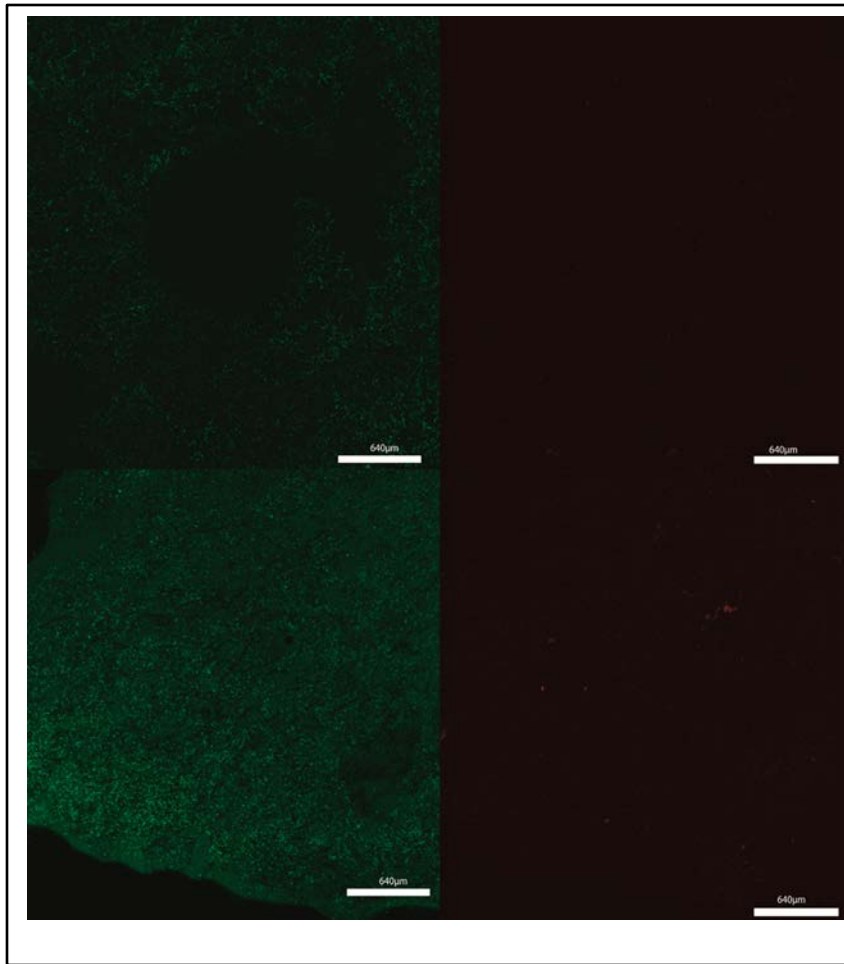
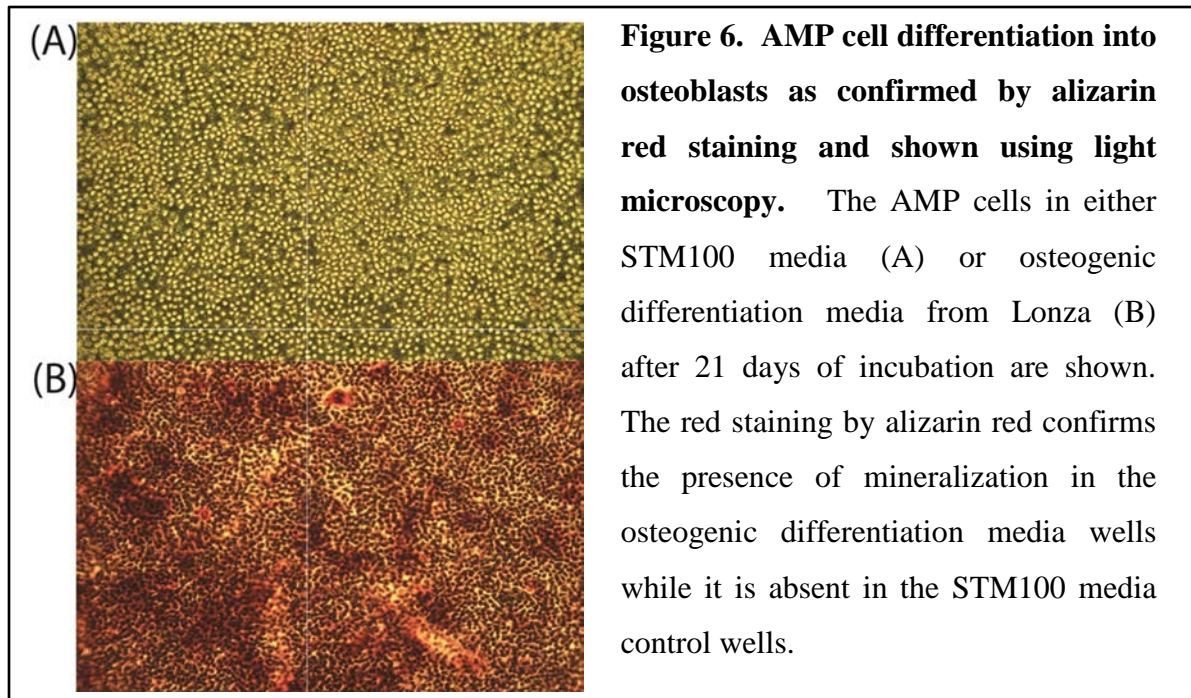


Figure 5. Confocal images of 1×10^6 AMP cells seeded onto Helistat® scaffold with live/dead fluorescent staining with a 640µm scale bar. Two-sided seeding resulted in viable AMP cells distributed throughout the scaffold. Cells penetrated about 0.5mm into the scaffold on the top side (top panels) and bottom side (bottom panels). Most of the cells remained viable as noted by the green dye. Few dead cells were observed as seen by the red dye.

AMP Cell Differentiation

As shown in Figure 6A, the cells in STM100 media for 21 days did not differentiate into osteoblasts or secrete calcium phosphate as indicated by the lack of alizarin red staining. However, as seen in Figure 6B, AMP cells incubated with osteogenic differentiation media for 21 days produced mineralization as shown by the amount of alizarin red staining. These data confirm that AMP cells possess the ability to differentiate into osteoblasts and induce mineralization.



Fluidigm Gene Expression

Gene expression of the defect area of the calvarial tissue of the treatment cohorts was analyzed by fluidigm analysis. Table 1 (at the end of the report) summarizes the data including genes that are differentially regulated significantly between time-points and groups. A total of 17 genes in the saline group, 19 genes in the ST266 group and eight genes in the AMP cell group were differentially regulated and were significantly different with respect to the one week time-point saline group. Genes which were significantly increased include *alkaline phosphatase*, *bglap*, *bmp3*, *bmp4*, *bmp5*, *gdf10* and *tgfb3*. The genes were significantly increased between the two week and six month time-points for all groups compared to the one week saline group (Table 1). In the saline group only, *bmp2*, *smad1*, *smad5* and *tgfb2* were additionally up-regulated significantly. When analyzing the two treatment groups, the ST266 group additionally had significantly up-regulated levels of *angpt1*, *bmp6*, *bmp7*, *coll14a1*, *fgf2* and *illa* over time, while in the AMP cell group, only *mmp8* was additionally up-regulated significantly (Table 1). Between the saline and ST266 groups, up-regulation over time was also seen for *bmpr1a*, *egf*, *fgf1*, *igf2*, *mmp10* and *runx2* (Table 1). When comparing between groups, expression of *col7a1* was significantly up-regulated at the two week time-point in the AMP cell group compared to the saline group, while levels of *gdf10* and *tgfb3* were significantly down-regulated in the AMP cell

group compared to the saline control. At the one month time-point, levels of *bmp3* and *bmp4* were significantly down-regulated in the AMP cell group compared to the saline group (Table 1). These data suggest that ST266 is not significantly influencing expression of genes related to the osteogenic differentiation pathways. Further, the AMP cell treatment appears to negatively influence osteogenic differentiation gene expression.

Microcomputed Tomography and Histology Evaluation

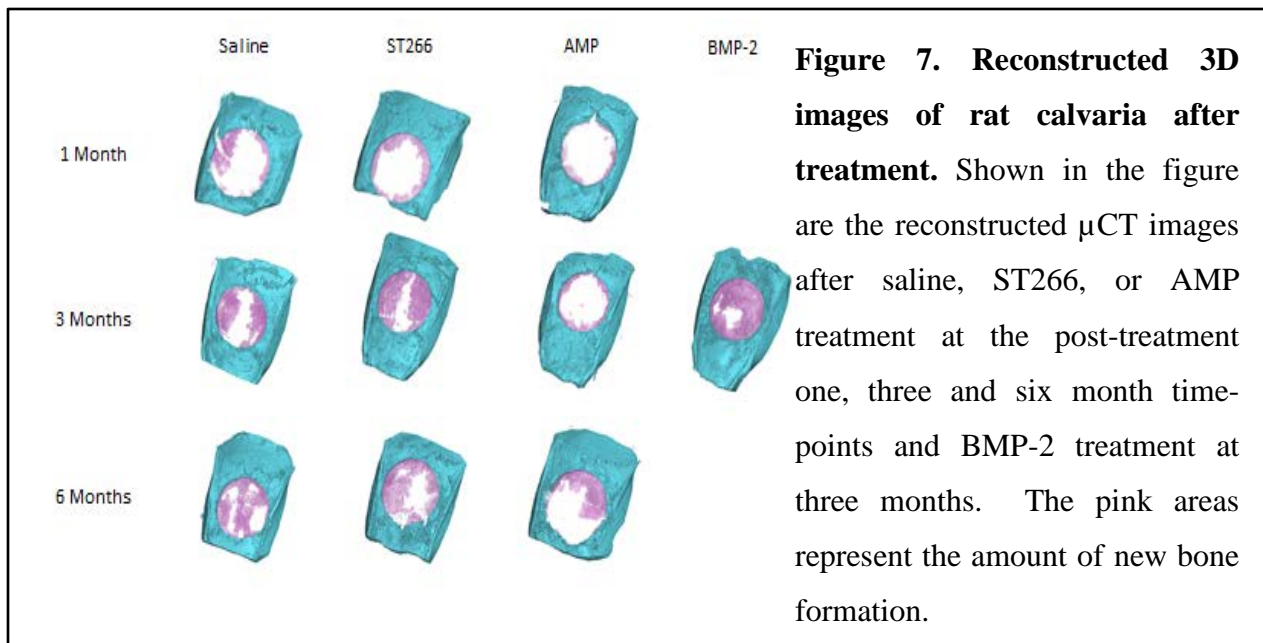
The 3-D reconstructed images of the μ CT data are shown in Figure 7. Quantitative μ CT analysis revealed that in terms of the bone volume regenerated, the bone volume increased in the saline group from one month ($14.61 \pm 2.60 \text{mm}^3$) to three months ($19.85 \pm 5.87 \text{mm}^3$) to six months ($26.86 \pm 8.35 \text{mm}^3$), while the bone volume with ST266 treatment significantly increased from one month ($12.75 \pm 8.30 \text{mm}^3$) to three months ($26.25 \pm 2.76 \text{mm}^3$), ending at $25.25 \pm 8.40 \text{mm}^3$ by six months. AMP cell treatment did not significantly increase bone volume/tissue volume (BV/TV) over time from one month ($7.54 \pm 1.84 \text{mm}^3$) to three months ($11.96 \pm 5.33 \text{mm}^3$) to six months ($11.01 \pm 3.79 \text{mm}^3$). Further, a significant increase in BV/TV with BMP-2 (our positive control) compared to the other three groups was observed at three months while a significant decrease in BV/TV was seen with AMP cells compared to controls at six months (Figure 8A).

Bone surface/bone volume (BS/BV) is indicative of bone turnover, which primarily occurs at the bone surface and is indicative of bone organization. Thus, the lower the BS/BV value, the more organized the bone. The BS/BV ratio decreased in all groups over time except for AMP cells from one month (44.77 ± 12.08 1/mm-saline; 55.72 ± 18.26 1/mm-ST266; 57.07 ± 17.33 1/mm-AMP cells) to three months (38.63 ± 15.74 1/mm-saline; 44.18 ± 12.72 1/mm-ST266; 96.48 ± 31.9 1/mm-AMP cells; 22.44 ± 3.84 1/mm-BMP-2) to six months (27.63 ± 5.28 1/mm-saline; 26.27 ± 4.35 1/mm-ST266; 38.63 ± 13.86 1/mm-AMP cells). At three months, the BS/BV ratio was significantly higher with the AMP cell treatment than the other groups (Figure 8B).

The Tb.pf is another measure of trabecular connectivity, organization and quality, which incorporates trabecular number, thickness and spacing. The lower the Tb.pf value, the more organized, connected and higher quality the newly formed bone. At one month, no significant differences were seen between groups (25.35 ± 10.09 1/mm-saline; 38.23 ± 19.75 1/mm-ST266; 43.3 ± 2.41 1/mm-AMP cells). By three months, Tb.pf was significantly lower with BMP-2 than

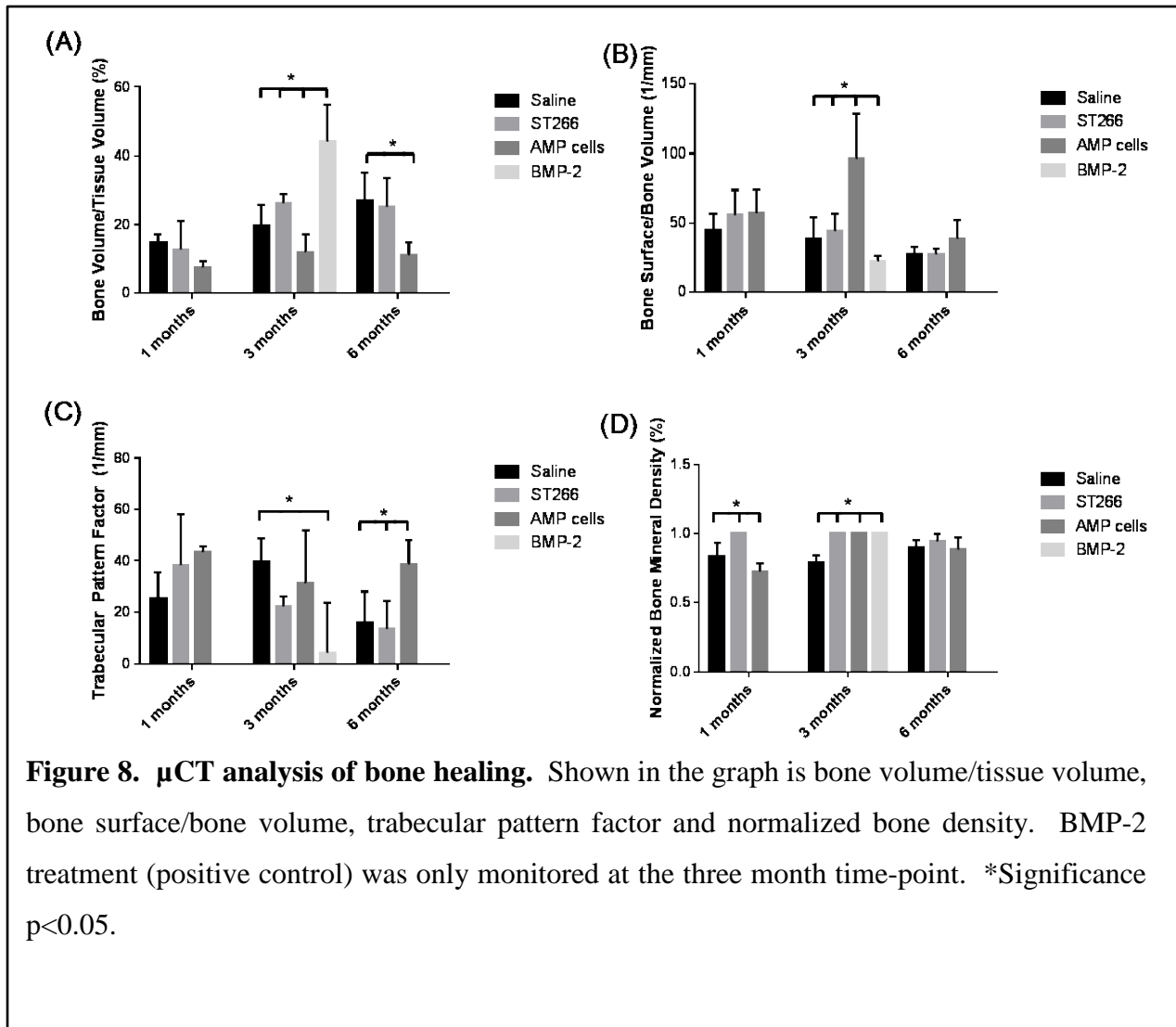
the saline group (39.62 ± 8.94 1/mm-saline; 22.09 ± 3.97 1/mm-ST266; 31.23 ± 20.49 1/mm-AMP cells; 4.43 ± 19.10 1/mm-BMP-2). While ST266 treatment did reduce Tb.pf by three months, it was not statistically significant (Figure 8C).

Normalized bone density reflects the overall density of the bone with 100% being the density of normal physiological bone and was significantly increased at one month with ST266 treatment ($100 \pm 0\%$) compared to saline ($83 \pm 10\%$) and AMP cell treatment ($72 \pm 6\%$). By three months, ST266 treatment, AMP cell treatment and BMP-2 treatment had significantly more bone density than saline treatment ($100 \pm 0\%$ for all three groups vs $78.75 \pm 5.76\%$ for saline). By six months, saline, ST266 and AMP cell treatments had similar amounts of bone density ($89.8 \pm 5.4\%$ for saline, $93.2 \pm 5.5\%$ for ST266 and $88.4 \pm 8.8\%$ for AMP cells) (Figure 8D).



Subgroup analysis was performed using a t-test with Welch's correction at the three month time-point between saline and ST266, which showed the greatest amount of change at the three month time-point. ST266 increased BV/TV compared to saline, but it was not statistically significant ($p=0.07$). There was no significant difference in BS/BV between groups. However, ST266 treatment did significantly lower Tb.pf compared to saline. Finally, ST266 treatment significantly increased bone density compared to saline at both the one and three month time-points.

The implant and area of newly regenerated bone were harvested and evaluated for the organization and cellular infiltration. Histological scoring of the calvaria from hematoxylin and eosin stained slides is shown in Table 2. The ST266 group had more defect closure, immature and mature new bone than the saline group by three months, as well as a significant increase in the amount of new blood vessels at one month (Figure 9). The saline group had more fibrovascular tissue compared to the ST266 group by three months. The AMP group had more fibrovascular tissue, less defect closure and less mature new bone formed than the saline and ST266 group at all time-points. By six months, both the ST266 and saline group were similar



while the AMP group continued to perform poorly compared to the other two groups.

Table 2. Histology scoring of rat calvaria.

Group	Time	Angiogenesis	Defect Closure (%)	New immature woven bone (%)	Fibrovascular tissue (%)	New mature lamellar bone (%)
Saline	1 month	2.20±0.45	1.40±0.55	2.60±0.55	1.60±0.55	0.40±0.55
ST266		3.00±0.00*	1.40±0.55	2.40±0.55	1.60±0.55	0.60±0.55
AMP		1.60±0.55	0.60±0.55	2.40±1.34	2.20±0.44	0.00±0.00
Saline	3 month	1.40±0.55	1.00±0.55	1.60±0.55	1.80±0.84	0.80±0.44
ST266		1.40±0.55	2.00±0.00	2.00±0.00	1.00±0.00	1.00±0.00
AMP		1.40±0.55	0.00±0.00	0.00±0.00	3.00±0.00	0.00±0.00
BMP-2		1.00±0.00	2.20±0.84	2.00±0.00	0.80±0.84	1.00±1.00
Saline	6 month	1.00±0.00	1.80±0.45	1.00±0.00	1.40±0.89	2.00±0.00
ST266		1.00±0.00	1.80±0.85	1.00±0.00	1.40±0.55	2.00±0.00
AMP		1.40±0.55	0.60±0.55	0.60±0.55	2.40±0.55	1.20±1.01

Histology scoring shown with mean +/- standard deviation. Angiogenesis refers to the amount of blood vessels present (0-none, 1-few new vessels, 2-many new vessels, 3-numerous new vessels). Degree of defect closure demonstrates amount of defect closed (0-none, 1-<50%, 2->50%, 3-100%). The % of new woven bone is the amount of new immature new bone formed (0-none, 1-<50%, 2->50%, 3-100%). The % of fibrovascular tissue refers to the amount fibrovascular tissue present in the defect (0-none, 1-<50%, 2->50%, 3-100%). The % of lamellar bone is the amount of new mature bone formed in the defect (0-none, 1-<50%, 2->50%, 3-100%).

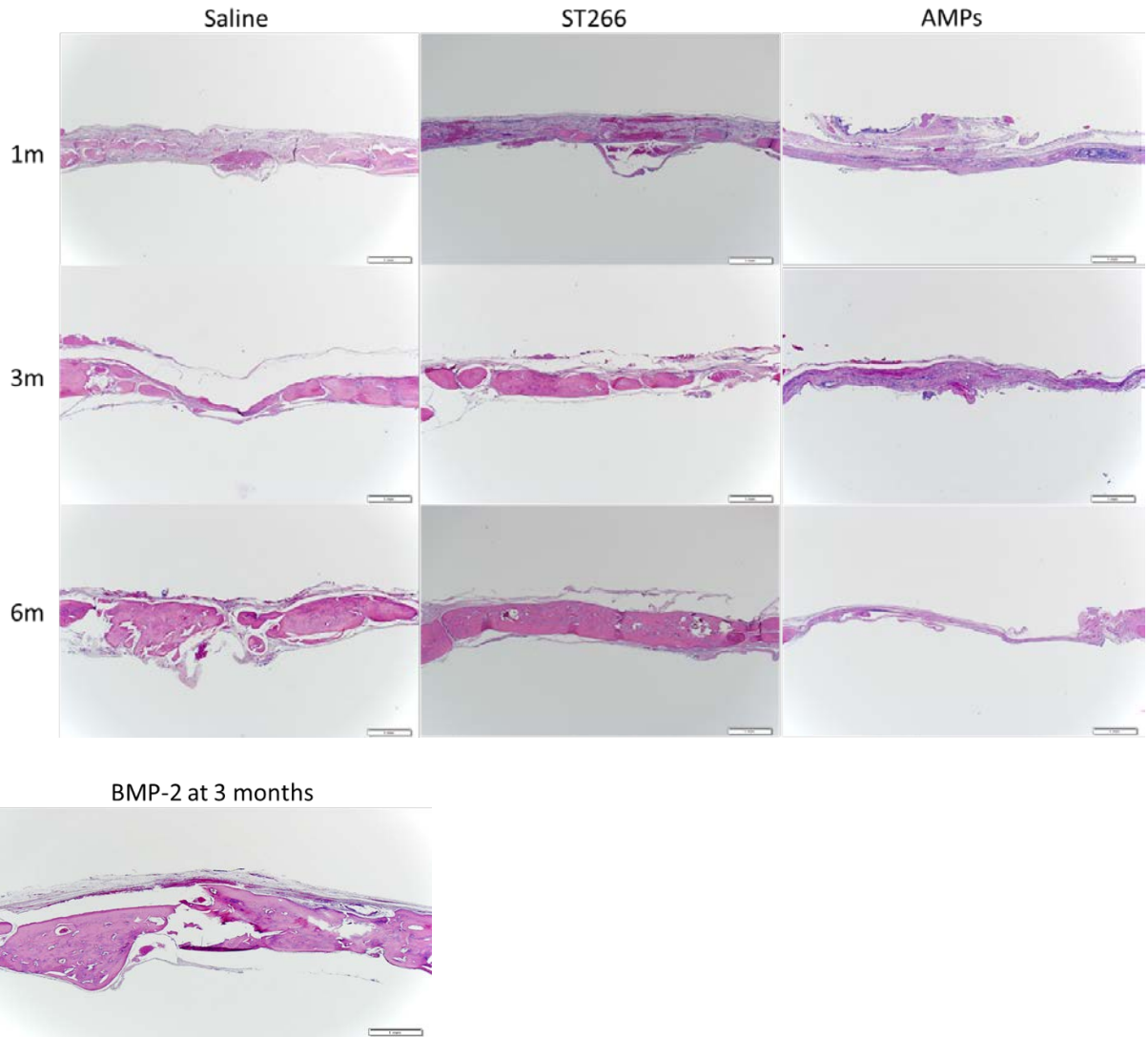


Figure 9. Shown in the figure is the cross-sectional area of the rat calvaria for the saline, ST266, BMP-2 and AMP cell groups at the one month, three month and six month time-points (100µm scale bar). New blood vessel formation is seen in the saline and ST266 groups at the one and three month time-points. New bone formation is evident with the saline and ST266 groups at all three time-points as well as the six month time-point showing the greatest amount of new bone formation. Additionally, new bone formation is evident in the BMP-2 group at the three month time-point. AMP cell treatment however, seemed to inhibit new bone formation which appeared to gradually resorb over time consistent with the µCT results.

DISCUSSION

Critical size bone defects induced by trauma continue to present a clinical challenge as autologous grafting remains the primary viable option for healing. With the limited availability of bone grafts, additional surgeries and prolonged inpatient care pose severe limitations on autologous bone grafting. These challenges have generated the need for alternative therapeutics that can repair critical size bone defects without the deleterious limitations of autologous grafting. In the present study, the ST266 treatment not only improved the proliferation and migration of bone-inducing cells *in vitro*, but also led to an improvement in overall new bone volume and quality, as demonstrated by increased mineralization and connectivity, as well as an increase in angiogenesis in the critical size defects *in vivo*. However, AMP cells, which naturally produce the ST266 secretome and can undergo osteogenic differentiation *in vitro*, did not promote bone regeneration and what little new bone formed was disorganized. Reasons for the poor performance of the AMP cells could be due to xeno-compatibility issues of human AMP cells in a rat model, or the release of different factors from the AMP cells when placed in an inflammatory environment *in vivo*.

The secretome derived from different tissue sources contains a number of growth factors that can enhance the migration, proliferation and even osteogenic induction of MSCs and osteoprogenitor cells [4-6, 20-22]. In this study, it was found that ST266 treatment led to a significant increase in the proliferation of both bone marrow-derived MSCs and osteoprogenitor cells as well as the migration of bone marrow-derived MSCs, both processes being critical to the formation of new bone [3, 10-13]. Similar results for proliferation and migration have also been shown when treating MSCs with the secretome derived from bone marrow-derived MSCs. The bone marrow-derived MSC secretome contains growth factors such as insulin growth factor-1 (IGF-1), VEGF, TGF β and hepatocyte growth factor, which have led to increased *in vivo* bone formation in rat calvarial defects as well [4, 5, 20]. Similarly, several growth factors have also been identified in ST266 that likely influence proliferation and migration including PDGF-BB, TGF β 2, VEGF, TIMP-1, TIMP-2 and angiogenin, although other unidentified factors such as exosomes may play a role as well [9, 23]. VEGF and angiogenin are potent inducers of angiogenesis and VEGF has also been shown to enhance proliferation and migration of osteoblasts [24, 25]. PDGF-BB and TGF β 2 enhance bone regeneration by acting as proliferative and chemotactic factors for MSCs, which are recruited to the defect site to differentiate into

osteoblasts [16, 17]. Finally, TIMP-2 has been shown to induce proliferation in primary rat calvarial osteoblast-like cell cultures as well as enhance healing in critical size bone defects [11]. Thus, the *in vitro* analysis demonstrated that ST266 has the potential to induce bone formation.

The μ CT analysis of bone regeneration in the calvarial defects revealed improvement of new bone formation with ST266 treatment as reflected by the increase in BV/TV compared to the saline controls by the 12 week time-point, although it was not significant. Importantly, ST266 treatment consistently improved the quality of bone healing as reflected by the increase in bone mineral density, which accounts for improved bone quality and lower Tb.pf values. Trabecular factor takes into account the overall trabecular organization and connectivity of the bone, with lower values representing more connected bone [26, 27]. Consistent with the μ CT results, histological scoring also demonstrated that, by 12 weeks, ST266 treatment groups had increased defect closure, increased immature and mature bone formation, and less fibrovascular tissue compared to the saline controls and AMP cells. Interestingly, another study investigating epidermal wound healing also found that ST266 improved the quality of healing. In that study, pig epidermal wounds treated with ST266 had a thicker epidermis and increased cell layers compared to controls, indicating that ST266 had improved the quality of wound healing in epidermal wounds [28], similar to the improvement in the quality of new bone formed in the present study.

Angiogenesis was also significantly enhanced at the four week time-point with ST266 treatment compared to saline controls and AMP cells, based on histological analysis. The importance of angiogenesis in bone regeneration is well-known as studies have found that large vascular injuries associated with fractures can lead to a rate of impaired healing that is as high as 46% [29]. Blood vessels carry the oxygen, nutrients, hormones and required proteins for bone regeneration while removing waste products [30], supporting their importance in bone healing. Factors in ST266 that may be contributing to the enhanced angiogenesis include VEGF, PDGF-BB and angiogenin, which are known angiogenic factors [31]. Thus, the improvement in bone regeneration observed with ST266 treatment may partly arise from the enhanced angiogenesis in combination with its osteo-inductive effects.

These results may have implications for the therapeutic potential of ST266 loaded scaffolds as a biotherapeutic in bone trauma, as well as diseases that can lead to eventual bone loss such as periodontitis (currently being evaluated in human clinical trials). A previous report

using ST266 treatment in a rabbit periodontal model revealed that ST266 treatment reduced inflammation and had increased new bone formation [32]. The increase in new bone formation may have arisen due to the reduction in chronic inflammation by ST266 treatment, thus allowing the initiation of osteogenesis. However, the results from our study suggest that ST266 treatment might also be improving the quality of new bone that formed. Thus, the utilization of ST266 treatment, not only might halt bone loss in diseases such as periodontitis, but could improve the quality of new bone that forms with increased mineralization and connectivity.

There are a few factors that could explain the lack of a statistically significant increase in new bone volume with ST266 treatment in the *in vivo* studies. The positive results of ST266 on the proliferation and migration of MSCs and proliferation of osteoprogenitor cells observed *in vitro* used the same amount of ST266 that was added to the scaffold for the *in vivo* studies. However, the MSCs and osteoprogenitor cells in the *in vitro* studies had continuous exposure to ST266 for a 48hr and 72hr time period. Conversely, according to the release kinetics, almost 50% of ST266 in the scaffold was released in the first day. Thus, the bone-forming cells that migrate to, and proliferate in the defect site *in vivo*, are only exposed to roughly 50% of ST266, since the migration and proliferation of bone-forming cells in the defect site occurs after the initial inflammatory phase (days one to three after injury) [33].

A burst release profile (~48% on day one) (Figure 3) was observed for ST266 release from the collagen scaffold, while the rest of the ST266 amount was retained between day one and 14 (less than 2 μ g ST266 released). Therefore, the remaining amount of proteins in ST266 still present in the collagen scaffold after day one were well below the therapeutic levels used in the *in vitro* studies and consequently, would result in low levels of ST266 proteins acting on the osteogenic cells at the calvarial defect site. Burst release profiles have exhibited a detrimental effect on therapeutic proteins in the past as higher therapeutic dosages must be incorporated into the scaffold to account for the initial burst release. For example, BMP-2 exhibits a similar burst release profile from the same collagen sponge, which results in the requirement for high BMP-2 dosage incorporation in the scaffold [34]. Unfortunately, the higher dosage also results in serious side effects such as inflammation and ectopic bone formation [35]. Thus, using a scaffold that exhibits a more controlled release of ST266 and/or incorporating a higher concentration of ST266 into the scaffold may further improve its osteo-inductive effects. One

possibility to address this issue could be to utilize hydrogels and/or 3D printing to better distribute and control the release of ST266 from the scaffold.

While therapeutics are being sought for healing critical size bone defects because they do not heal on their own, therapeutics that can speed up the healing of non-critical size bone defects are still of interest and importance. In this study, the osteo-inductive effect of ST266, as a biotherapeutic, was investigated in a critical size bone defect. While the amount of ST266 used in this study may not have been enough (due to a low initial dosage amount and/or burst release profile) to fully heal a critical size bone defect, it may have been sufficient for accelerating healing and improving the quality of bone formation in a non-critical size defect. Thus, it would be worthwhile to determine if ST266 may serve as a viable therapeutic for accelerating the healing and improving the quality of bone formation in non-critical size bone defects such as isolated vertical periodontal defects or extraction sites. As incorporating ST266 in the scaffolds resulted in improved bone quality compared to AMP cells, ST266 should be the focus of future studies.

Overall, the results of this study using ST266 at the current concentration demonstrated beneficial effects on the proliferation of MSCs and osteoprogenitor cells and increased migration of MSCs *in vitro*. ST266 treatment improved the quality and amount of bone regeneration and angiogenesis with no deleterious effects observed. Although the amount of new bone formation was not statistically significant with ST266 treatment compared to controls, it was consistently higher and did result in a statistically significant improvement in the mineralization of new bone compared to controls as well as result in a significant increase in angiogenesis. AMP cells however, appeared to inhibit bone formation. The inhibition of AMP cells could have been due to a xeno-compatibility issue or expression of different inhibitor factors since they were exposed to an inflammatory environment. In conclusion, ST266 could be a viable biotherapeutic for bone regeneration and further studies are certainly warranted. Improvements could be made including utilizing a higher dose of ST266 in the scaffold, as well as improving the release kinetics of ST266 from the scaffold.

MILITARY SIGNIFICANCE

As of October 2014, the wars in Iraq and Afghanistan have resulted in substantial morbidity and mortality including a total of 6,820 deaths and 52,281 wounded in action during Operation Iraqi Freedom, Operation New Dawn and Operation Enduring Freedom combined [36]. Due to the nature of combat injuries caused by improvised explosive devices, mortars, rocket-propelled grenades and gunshots sustained by military personnel in protective gear, extremity wounds, including the head, neck and face, continue to rise relative to other types of injury. Craniomaxillofacial injuries incurred by warfighters often result in massive bone tissue destruction. Unfortunately, the current standards of care for craniomaxillofacial bone regeneration have significant disadvantages including prohibitive costs, graft rejection and prolonged hospitalization [37]. Thus, the identification of readily available, low-cost therapeutics capable of regenerating bone with minimal side effects is critically needed for the effective treatment of military personnel suffering from craniomaxillofacial bone injuries. The beneficial effects of ST266 identified in this report on bone defects should be further optimized and could be a viable therapeutic for surgeons to use as a therapeutic for warfighters subjected to severe bone trauma defects.

Table 1. Significant gene expression changes across time and treatment groups.

Gene	1 WEEK						2 WEEK						1 MONTH					
	SAL	s.d	ST266	s.d	AMP	s.d	SAL	s.d	ST266	s.d	AMP	s.d	SAL	s.d	ST266	s.d	AMP	s.d
Alp	1.0	0	1.2	0.2	1.5	1.0	2.1	0.9	3.2	3.2	1.4	1.1	4.6*	3.5	2.9	0.7	2.7	2.2
Angpt1	1.0	0	0.8	0.2	1.6	1.7	1.3	0.6	2.9	2.9	1.3	1.0	2.2	1.3	2.4	1.1	1.9	1.6
Bglap	1.0	0	1.0	0.3	1.9	1.8	3.8	1.7	4.2	4.3	2.4	1.7	7.2*	5.2	8.3*	2.4	5.6	3.4
Bmp2	1.0	0	1.5	0.5	7.4	10.1	2.8	1.4	8.1	11.8	2.5	2.0	7.5	11.2	8.5	5.4	2.6	1.8
Bmp3	1.0	0	0.9	.04	1.9	0.4	3.0*	0.8	2.6	1.3	1.6	0.4	8.9*	2.7	5.7*	1.2	3.4[®]	0.8
Bmp4	1.0	0	0.6	0.2	2.0	2.7	2.0	0.5	1.5	1.1	1.0	0.7	6.8*	3.9	2.9*	0.2	1.8[®]	1.3
Bmp5	1.0	0	1.0	0.4	3.6	5.3	2.8	1.5	3.0	2.5	1.0	1.1	6.1	4.7	3.5	1.2	2.4	2.1
Bmp6	1.0	0	0.5	0.3	4.5	7.4	2.7	2.3	4.4	5.5	0.9	1.2	8.4	13.3	3.2	0.7	3.0	4.2
Bmp7	1.0	0	0.6	0.6	12.3	20.8	1.6	0.5	1.0	0.8	2.3	2.2	11.0	11.3	4.5	1.6	4.4	5.6
Bmpr1a	1.0	0	0.8	.05	2.4	2.7	2.0	0.8	2.5	2.7	1.5	1.0	4.9*	2.8	3.0	1.1	2.2	1.5
Col7a1	1.0	0	1.4	0.8	4.5	6.8	0.4	0.4	1.2	0.6	2.8[®]	2.1	0.6	0.4	0.4	0.1	0.4	0.3
Col14a1	1.0	0	0.5	0.1	0.5	.02	1.3	0.3	1.8	1.7	1.1	0.9	1.7	1.0	1.6*	0.5	1.1	0.6
Egf	1.0	0	1.1	0.8	2.7	3.3	2.4	1.3	3.0	3.6	1.4	1.2	8.3	8.4	3.2	0.3	2.8	3.0
Fgf1	1.0	0	1.0	0.8	3.0	4.2	2.3	1.1	2.4	2.7	0.9	0.7	6.5	4.7	4.3	0.8	6.8	7.9
Fgf2	1.0	0	1.1	0.3	0.9	0	1.7	0.4	1.1	0.1	1.7	0.6	2.6	0.8	2.7	0.2	1.4	0.7
Gdf10	1.0	0	1.2	0.1	5.5	5.9	11.3*	5.1	8.4	11.8	3.0[®]	3.3	54.5*	60.8	26.4*	22.7	12.0	7.4
Igf2	1.0	0	0.6	0.5	1.3	1.7	2.0	0.8	2.6	2.6	1.1	1.3	5.2	2.0	4.0*	2.8	2.3	2.0
IL1a	1.0	0	27.8	44.6	26.4	45.2	0.2	.09	0.9	.06	12.1	16.5	0.1	0.1	0.3	0.2	0.1	.08
Mmp8	1.0	0	4.8	6.9	7.9	11.0	1.1	1.5	2.0	1.7	2.0	1.6	0.5	0.5	1.3	1.3	2.3	3.6
Mmp10	1.0	0	0.6	.08	2.2	1.9	1.8	1.3	5.7	7.8	4.5	3.2	7.3	9.3	3.4	1.7	1.7	1.4
Smad1	1.0	0	1.1	0.3	7.5	11.6	1.8	0.9	7.6	11.6	3.0	3.2	6.3	8.8	4.6	4.0	1.7	1.4
Smad5	1.0	0	0.9	0.2	4.6	6.5	1.7	0.9	5.1	7.2	2.2	2.3	4.2	4.8	3.6	2.2	1.7	1.3
Runx2	1.0	0	1.1	.04	3.0	3.4	1.8	0.6	3.8	4.6	1.8	1.3	4.5	4.4	4.1	2.4	2.4	1.3
Tgfb2	1.0	0	1.1	0.5	8.0	12.2	2.6	1.5	4.1	5.5	2.0	2.1	8.3	10.3	5.8	3.0	3.7	3.5
Tgfb3	1.0	0	0.7	.07	1.8	1.4	3.2*	1.2	2.1	1.9	1.0[®]	0.7	5.2*	1.7	3.4*	1.6	2.6	1.4

Table 1 continued

Gene	3 MONTH						6 MONTH					
	SAL	s.d	ST266	s.d	AMP	s.d	SAL	s.d	ST266	s.d	AMP	s.d
Alp	4.5*	1.9	4.8*	1.9	5.4*	2.3	8.9*	0.4	7.1*	3.2	7.2*	0
Angpt1	2.6	1.0	3.8*	1.4	3.0	1.4	4.7	1.7	6.0*	5.6	7.0	0
Bglap	3.9*	0.3	6.1*	2.3	8.5*	4.8	10.8*	0.5	6.5*	4.0	4.4	0
Bmp2	1.3	0.2	4.1	2.3	4.9	4.3	12.5*	2.1	8.6	7.2	2.3	0
Bmp3	9.6*	3.1	6.3*	1.9	10.3*	2.9	20.0*	5.2	8.2*	2.1	10.6*	0
Bmp4	4.8*	1.4	6.7*	2.9	8.4*	6.5	10.6*	3.8	9.1*	3.5	4.8	0
Bmp5	8.0*	4.0	7.3*	2.1	11.5*	7.1	19.4*	4.3	15.9*	11.2	22.6*	0
Bmp6	2.8	2.9	20.0*	10.9	22.4	25.6	13.8	12.8	10.7	7.0	6.4	0
Bmp7	7.2	5.3	15.0*	7.8	23.5	33.0	18.8	5.2	24.0*	20.9	6.8	0
Bmpr1a	3.2	1.4	4.4*	1.5	2.1	3.3	9.8*	6.0	6.2*	3.1	5.0	0
Col7a1	0.8	0.6	0.8	0.3	1.1	1.1	1.3	1.2	1.4	0.4	0.6	0
Col14a1	0.6	.05	1.3	0.5	1.1	0.3	1.4	0.1	0.8	0.3	1.0	0
Egf	3.7	1.7	7.0	2.1	8.1	6.7	32.0*	30.0	16.7*	14.3	5.2	0
Fgf1	5.4	4.3	11.0*	4.6	11.8	11.9	48.5*	46.9	19.4*	6.3	5.1	0
Fgf2	1.6	0.5	2.0*	1.6	1.8	0.4	1.5	1.0	0.4	.06	0.6	0
Gdf10	19.2*	5.6	38.7*	12.4	46.4*	36.2	160.7*	34.8	35.4*	14.9	32.5	0
Igf2	3.3	3.8	6.5*	2.2	4.2	1.9	10.4*	1.4	5.7*	4.5	2.3	0
IL1a	0.3	0.2	0.5	0.8	0.5	0.4	0.3	.05	0.2*	.08	0.1	0
Mmp8	1.1	0.5	0.9	0.4	0.4*	0.4	4.1	2.8	11.6	14.0	0.6	0
Mmp10	3.6	0.8	4.1	2.4	4.0	1.7	21.8*	16.4	6.3*	5.2	3.4	0
Smad1	1.4	0.7	3.4	1.5	4.2	3.0	14.8*	0.9	5.6	4.8	1.5	0
Smad5	1.8	0.3	3.3	1.6	4.1	2.8	11.5*	4.3	4.8	1.7	2.1	0
Runx2	2.9	0.9	3.0	1.1	3.6	2.4	10.3*	3.9	5.4*	1.9	3.2	0
Tgfb2	2.7	1.1	5.6	3.0	6.1	4.9	21.4*	10.6	9.3	5.0	3.0	0
Tgfb3	2.6	0.6	3.2*	0.2	4.4*	0.9	6.4*	1.4	3.3*	0.9	3.4	0

Table 1. Gene expression displayed as mean fold change is shown with \pm standard deviation (s.d). Data was normalized to the one week saline group. Groups include saline (SAL), ST266 and amnion-derived multipotent progenitor (AMP) cell treated at each time-point. Time-points include one week, two weeks, one month, three months and six months post-surgery. All groups included three animals except for the six month SAL group which had two animals and the six month AMP group which had one animal due to low RNA yield and purity. * is significance between the one week time-point vs. the other time-points for that treatment. The @ is significance between the AMP cell group and the saline group for that particular time point; p<0.05 significance.

REFERENCES

1. Kalfas, I.H., *Principles of bone healing*. Neurosurg Focus, 2001. **10**(4): p. E1.
2. Oryan, A., et al., *Bone regenerative medicine: classic options, novel strategies, and future directions*. J Orthop Surg Res, 2014. **9**(1): p. 18.
3. Wang, X., et al., *Role of mesenchymal stem cells in bone regeneration and fracture repair: a review*. Int Orthop, 2013. **37**(12): p. 2491-8.
4. Katagiri, W., et al., *Novel cell-free regeneration of bone using stem cell-derived growth factors*. Int J Oral Maxillofac Implants, 2013. **28**(4): p. 1009-16.
5. Osugi, M., et al., *Conditioned media from mesenchymal stem cells enhanced bone regeneration in rat calvarial bone defects*. Tissue Eng Part A, 2012. **18**(13-14): p. 1479-89.
6. Linero, I. and O. Chaparro, *Paracrine effect of mesenchymal stem cells derived from human adipose tissue in bone regeneration*. PLoS One, 2014. **9**(9): p. e107001.
7. Pawitan, J.A., *Prospect of stem cell conditioned medium in regenerative medicine*. Biomed Res Int, 2014. **2014**: p. 965849.
8. Hass, R., et al., *Different populations and sources of human mesenchymal stem cells (MSC): A comparison of adult and neonatal tissue-derived MSC*. Cell Commun Signal, 2011. **9**: p. 12.
9. Steed, D.L., et al., *Amnion-derived cellular cytokine solution: a physiological combination of cytokines for wound healing*. Eplasty, 2008. **8**: p. e18.
10. De la Riva, B., et al., *Local controlled release of VEGF and PDGF from a combined brushite-chitosan system enhances bone regeneration*. J Control Release, 2010. **143**(1): p. 45-52.
11. Kramer, F.J., et al., *Tissue inhibitor of metalloproteinases II (TIMP-2) is an osteoanabolic factor in vitro and in vivo*. Eur J Med Res, 2008. **13**(6): p. 292-8.
12. Kishimoto, K., et al., *Endogenous angiogenin in endothelial cells is a general requirement for cell proliferation and angiogenesis*. Oncogene, 2005. **24**(3): p. 445-56.
13. Xu, L., et al., *The healing of critical-size calvarial bone defects in rat with rhPDGF-BB, BMSCs, and beta-TCP scaffolds*. J Mater Sci Mater Med, 2012. **23**(4): p. 1073-84.
14. Leach, J.K., et al., *Coating of VEGF-releasing scaffolds with bioactive glass for angiogenesis and bone regeneration*. Biomaterials, 2006. **27**(17): p. 3249-55.
15. Yang, Y.Q., et al., *The role of vascular endothelial growth factor in ossification*. Int J Oral Sci, 2012. **4**(2): p. 64-8.
16. Phipps, M.C., Y. Xu, and S.L. Bellis, *Delivery of platelet-derived growth factor as a chemotactic factor for mesenchymal stem cells by bone-mimetic electrospun scaffolds*. PLoS One, 2012. **7**(7): p. e40831.
17. Poniatowski, L.A., et al., *Transforming growth factor Beta family: insight into the role of growth factors in regulation of fracture healing biology and potential clinical applications*. Mediators Inflamm, 2015. **2015**: p. 137823.
18. Spicer, P.P., et al., *Evaluation of bone regeneration using the rat critical size calvarial defect*. Nat Protoc, 2012. **7**(10): p. 1918-29.
19. Gibson-Corley, K.N., A.K. Olivier, and D.K. Meyerholz, *Principles for valid histopathologic scoring in research*. Vet Pathol, 2013. **50**(6): p. 1007-15.
20. Chang, W., et al., *Enhanced Healing of Rat Calvarial Bone Defects with Hypoxic Conditioned Medium from Mesenchymal Stem Cells through Increased Endogenous Stem Cell Migration via Regulation of ICAM-1 Targeted-microRNA-221*. Mol Cells, 2015. **38**(7): p. 643-50.
21. Shen, C., et al., *Conditioned medium from umbilical cord mesenchymal stem cells induces migration and angiogenesis*. Mol Med Rep, 2015. **12**(1): p. 20-30.
22. Wang, K.X., et al., *The effects of secretion factors from umbilical cord derived mesenchymal stem cells on osteogenic differentiation of mesenchymal stem cells*. PLoS One, 2015. **10**(3): p. e0120593.

23. Qin, Y., et al., *Exosome: A Novel Approach to Stimulate Bone Regeneration through Regulation of Osteogenesis and Angiogenesis*. Int J Mol Sci, 2016. **17**(5).
24. Mayr-Wohlfart, U., et al., *Vascular endothelial growth factor stimulates chemotactic migration of primary human osteoblasts*. Bone, 2002. **30**(3): p. 472-7.
25. Sheng, J. and Z. Xu, *Three decades of research on angiogenin: a review and perspective*. Acta Biochim Biophys Sin (Shanghai), 2016. **48**(5): p. 399-410.
26. Hahn, M., et al., *Trabecular bone pattern factor—a new parameter for simple quantification of bone microarchitecture*. Bone, 1992. **13**(4): p. 327-330.
27. Jonasson, G., G. Bankvall, and S. Kiliaridis, *Estimation of skeletal bone mineral density by means of the trabecular pattern of the alveolar bone, its interdental thickness, and the bone mass of the mandible*. Oral Surgery, Oral Medicine, Oral Pathology, Oral Radiology, and Endodontology, 2001. **92**(3): p. 346-352.
28. Bergmann, J., et al., *The effect of amnion-derived cellular cytokine solution on the epithelialization of partial-thickness donor site wounds in normal and streptozotocin-induced diabetic swine*. Eplasty, 2009. **9**: p. e49.
29. Dickson, K.F., S. Katzman, and G. Paiement, *The importance of the blood supply in the healing of tibial fractures*. Contemp Orthop, 1995. **30**(6): p. 489-93.
30. Saran, U., S. Gemini Piperni, and S. Chatterjee, *Role of angiogenesis in bone repair*. Arch Biochem Biophys, 2014. **561**: p. 109-17.
31. Stegen, S., N. van Gastel, and G. Carmeliet, *Bringing new life to damaged bone: the importance of angiogenesis in bone repair and regeneration*. Bone, 2015. **70**: p. 19-27.
32. Goo, B.J., *Host-modulating therapeutic approaches in periodontal disease: histological evaluations [M.S Thesis]*. School of Medicine, 2015. **Boston, University, Boston, MA**.
33. Dimitriou, R., E. Tsiridis, and P.V. Giannoudis, *Current concepts of molecular aspects of bone healing*. Injury, 2005. **36**(12): p. 1392-404.
34. Yang, H.S., et al., *Comparison between heparin-conjugated fibrin and collagen sponge as bone morphogenetic protein-2 carriers for bone regeneration*. Exp Mol Med, 2012. **44**(5): p. 350-5.
35. Bhakta, G., et al., *The influence of collagen and hyaluronan matrices on the delivery and bioactivity of bone morphogenetic protein-2 and ectopic bone formation*. Acta Biomater, 2013. **9**(11): p. 9098-106.
36. Fischer, H., *A Guide to U.S Military Casualty Statistics: Operation Inherent Resolve, Operation New Dawn, Operation Iraqi Freedom, and Operation Enduring Freedom*. Congressional Research Service, 2014. **7-5700**(RS22452): p. 1-9.
37. Kinoshita, Y. and H. Maeda, *Recent developments of functional scaffolds for craniomaxillofacial bone tissue engineering applications*. ScientificWorldJournal, 2013. **2013**: p. 863157.

REPORT DOCUMENTATION PAGE

The public reporting burden for this collection of information is estimated to average 1 hour per response, including the time for reviewing instructions, searching existing data sources, gathering and maintaining the data needed, and completing and reviewing the collection of information. Send comments regarding this burden estimate or any other aspect of this collection of information, including suggestions for reducing the burden, to Washington Headquarters Services, Directorate for Information Operations and Reports, 1215 Jefferson Davis Highway, Suite 1204, Arlington, VA 22202-4302, Respondents should be aware that notwithstanding any other provision of law, no person shall be subject to any penalty for failing to comply with a collection of information if it does not display a currently valid OMB Control number. **PLEASE DO NOT RETURN YOUR FORM TO THE ABOVE ADDRESS.**

1. REPORT DATE (DD MM YY) 10 10 17	2. REPORT TYPE Technical Report	3. DATES COVERED (from – to) April 2015 – April 2017
--	---	--

4. TITLE Evaluation of Amnion-derived Multipotent Progenitor (AMP) Cells and Amnion-derived Cellular Cytokine Solution (ST266) in Promoting Craniomaxillofacial Regenerative Bone Healing in Critical Size Calvarial Defects	5a. Contract Number: 5b. Grant Number: 5c. Program Element Number: 5d. Project Number: 5e. Task Number: 5f. Work Unit Number: G1507
--	--

6. AUTHORS Stukel, Jessica M. PhD, Guda, Teja PhD, Thompson, Michelle E. DVM, Banas, Richard M.S, Sheppard, Forest M.D, Burdette, Alexander J. PhD	
--	--

7. PERFORMING ORGANIZATION NAME(S) AND ADDRESS(ES) Naval Medical Research Unit San Antonio, Department of Expeditionary and Trauma Medicine, JBSA-Fort Sam Houston, TX	
--	--

8. SPONSORING/MONITORING AGENCY NAMES(S) AND ADDRESS(ES) Naval Medical Research Center, Advanced Medical Development 503 Robert Grant Avenue Silver Spring, MD 20910	8. PERFORMING ORGANIZATION REPORT NUMBER Report No. 2018-08
--	---

	10. SPONSOR/MONITOR'S ACRONYM(S) NMRC AMD
--	---

	11. SPONSOR/MONITOR'S REPORT NUMBER(S)
--	---

12. DISTRIBUTION/AVAILABILITY STATEMENT Approved for public release; distribution is unlimited.

13. SUPPLEMENTARY NOTES

14. ABSTRACT Traumatic injuries often result in critical size bone defects that are unable to heal without treatment. While autologous grafting is the standard of care, it has disadvantages that cell-based and biotherapeutic strategies aim to address. Amnion-derived multipotent progenitor (AMP) cells release ST266, a secretome of biomolecules integral to bone regeneration and angiogenesis. The objective was to determine the regenerative potential of AMP cells and ST266 in healing critical size bone defects in a rat model and use gene analytics to establish a mechanism for pro-osteogenic effects. ST266 enhanced proliferation and migration of MSCs and the proliferation of osteoprogenitor cells <i>in vitro</i> . AMP cells showed slight osteogenic differentiation and good viability on the scaffold. ST266 improved new bone volume and connectivity by 12 weeks, significantly improved angiogenesis at four weeks and bone density at four and 12 weeks with no deleterious effects. ST266 was superior to the AMP cells as the AMP cells appeared to inhibit bone formation. Fluidigm gene analysis showed up-regulation of osteogenic-related genes over time in all groups but no significant differences between groups. Improvement in new bone volume, connectivity and angiogenesis suggests that ST266 is beneficial for bone healing and a higher dose of ST266 may further improve regeneration.

15. SUBJECT TERMS ST266, AMP cells, craniomaxillofacial bone regeneration, critical size defects
--

16. SECURITY CLASSIFICATION OF: U	17. LIMITATION OF ABSTRACT UNCL	18. NUMBER OF PAGES 35	18a. NAME OF RESPONSIBLE PERSON CAPT Thomas Herzig, Commanding Officer
a. REPORT UNCL	b. ABSTRACT UNCL	c. THIS PAGE UNCL	18b. TELEPHONE NUMBER (INCLUDING AREA CODE) COMM/DSN: 210-539-5334 (DSN: 389)